Molecule-Based Magnets

DOI: 10.1002/anie.200802574

An Electron-Transfer Ferromagnet with $T_c = 107$ K Based on a Three-Dimensional $[Ru_2]_2$/TCNQ System**

Natsuko Motokawa, Hitoshi Miyasaka, Masahiro Yamashita, and Kim R. Dunbar*

The design of dπ–pπ molecular systems with efficient electronic communication is a long-standing goal in the field of inorganic chemistry. Guiding principles for this research are provided by the seminal studies on the Creutz–Taube ion, $[(H_3N)_5Ru(\mu\text{-pyz})Ru(NH_3)_5]^{5+}$ (pyz = pyrazine), discovered in 1969,[1] as well as subsequent related compounds[2] that undergo charge-transfer interactions between mixed-valent metal ions through an organic bridging ligand. Various experimental investigations to evaluate the electron-transfer dynamics were undertaken and theoretical interpretations from kinetic and, thermodynamic approaches were developed by Hush,[3] Marcus and Sutin,[4] and others.[5]

In the context of the current work, we also note the important contributions of Crutchley and co-workers, who explored electron-transfer processes in dinuclear ruthenium(III) complexes bridged by the 1,4-dicyanamidobenzene dianion ($Dicyd^{2-}$) or one of its substituted derivatives.[6] Interestingly, this class of compounds demonstrated strong intramolecular magnetic coupling between Ru^{III} $S = 1/2$ spins via the pπ orbital of the Dicyd bridge with J exceeding 400 cm^{-1} closely associated with a highly conjugated π–d network, classified as Class II or III behavior on the Robin–Day scale.[7] A crucial design ingredient for such systems is a 1:2 ratio of the one-electron donor (D, i.e., Dicyd) to the one-electron acceptor (A, i.e., a Ru^{III} ion) that can lead to an electron-transfer resonance of type $[A^-\text{–}D^+\text{–}A \leftrightarrow A\text{–}D\text{–}A \leftrightarrow A\text{–}D^+\text{–}A^-]$, in much the same fashion that the Creutz–Taube ion can exist in two resonance forms $[Ru^{III}\text{-pyz-}Ru^{II} \leftrightarrow Ru^{II}\text{-pyz-}Ru^{III}]$.

Our research is directed at the synthesis of coordination framework solids with dπ/pπ conjugation with the goal of achieving hybrid magnetic and conducting properties. In short, our research in this area can be expressed conceptually as "expanding the Creutz–Taube molecule to higher dimensions". The strategy is to design networks with a D:A ratio of 2:1 or 1:2 which involve a one-electron transfer that "turns on" electron-transfer resonance. In this vein, we chose to study the family of paddlewheel-type diruthenium(II,II) complexes with $S = 1$ as an electron donor to undergo the reversible redox reaction $[Ru_2^{II,II}] \leftrightarrow [Ru_2^{II,III}]$ without a significant change of structure.[8] The molecule concomitantly acts as a linear building block,[9] with 7,7,8,8-tetracyanoquinodimethane (TCNQ) acting as an electron acceptor and tetrakis-monodentate donor ligand. In earlier work, the 2:1 assemblies $[\{Ru_2(O_2CCF_3)\}_2TCNQ]\cdot 3\,S$ (S = toluene, **1a**;[10] *p*-xylene, **1b**)[11] and $[\{Ru_2(O_2CCF_3)\}_2TCNQF_4]\cdot 3\,p\text{-xylene}$ ($TCNQF_4$ = 2,3,5,6-tetrafluoro-7,7,8,8-tetracyanoquinodimethane; **2**),[11] with two-dimensional (2D) fishing-net-like (hexagonal) layered structures (Figure 1) were synthesized. While **1a** and **1b** showed poor if any $[Ru_2] \rightarrow$ TCNQ electron transfer, **2** exhibited significant electron-transfer resonance which led to unusual magnetic properties, that is, the compound is a metamagnet with $T_N = 95$ K (a field-induced ferromagnet), albeit not the high-T_c ferromagnet that we were seeking.

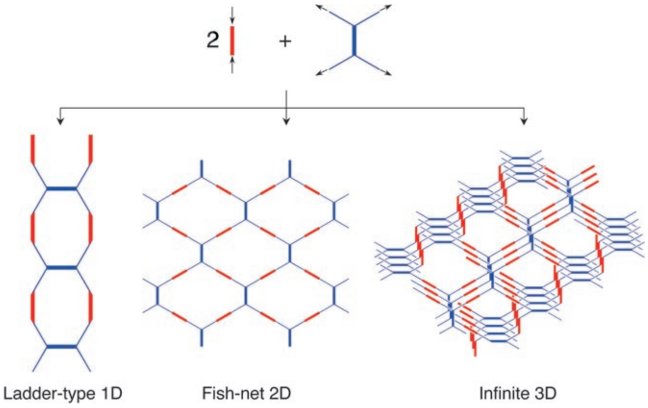

Figure 1. Possible structural types for $[Ru_2]_2$/TCNQ assemblies.

Herein we report a new structural type of the $[Ru_2]_2$/TCNQ system which is an infinite (3D) network in contrast to the 2D layer[10,11] or ladder chain[12] motifs reported earlier (Figure 1): $[\{Ru_2(O_2CPh\text{-}m\text{-}F)_4\}_2(\text{BTDA-TCNQ})]$ (**3**; *m*-F-$PhCO_2^-$ = *m*-fluorobenzoate, BTDA-TCNQ = bis(1,2,5-thiadiazolo)tetracyanoquinodimethane). The new compound exhibits a long-range ferromagnetic transition at $T_c = 107$ K.

Crystals of **3** were prepared by diffusion of layered solutions of BTDA-TCNQ in CH_2Cl_2 (bottom layer) and $[Ru_2(O_2CPh\text{-}m\text{-}F)_4(THF)_2]$ in 4-chlorotoluene (top layer) in a narrow-diameter glass tube (∅ 8 mm) under anaerobic

---

[*] N. Motokawa, Prof. Dr. H. Miyasaka, Prof. Dr. M. Yamashita
Department of Chemistry, Graduate School of Science
Tohoku University
6-3 Aramaki-Aza-Aoba, Aoba-ku, Sendai, Miyagi 980-8578 (Japan)
Fax: (+81) 22-795-6548
E-mail: miyasaka@agnus.chem.tohoku.ac.jp

Prof. Dr. K. R. Dunbar
Department of Chemistry, Texas A&M University
PO Box 30012, College Station, TX 77842-3012 (USA)

[**] This work was supported by a Grant-in-Aid for Scientific Research from the Ministry of Education, Culture, Sports, Science, and Technology (Japan) and The Asahi Glass Foundation (H.M.). K.R.D. thanks the National Science Foundation Chemistry Division for financial support.

Supporting information for this article is available on the WWW under http://dx.doi.org/10.1002/anie.200802574.

conditions. Compound **3** crystallizes in the monoclinic space group $C2/c$, and the asymmetric unit comprises two unique $[Ru_2(O_2CPh\text{-}m\text{-}F)_4]$ units and one BTDA-TCNQ molecule, both of which reside on an inversion center ($Z=4$). Figure 2 depicts a thermal ellipsoid plot and a packing diagram of **3**. The BTDA-TCNQ moiety in **3** acts as a μ_4-bridging group, as was found for **1** and **2** with TCNQ and $TCNQF_4$, respectively. In this arrangement, two axial coordination sites of respective $[Ru_2]$ units are used to provide the links to form the neutral network. While **1** and **2** exhibit a 2D hexagonal network,[10,11] **3** is an infinite 3D network structure (Figure 2b). All TCNQ and $TCNQF_4$ molecules in **1** and **2** are identical and orientated in a plane in a parallel manner, whereas the BTDA-TCNQ molecules in **3** adopt two orientations, namely, parallel to the $b+c$ axis and $b-c$ axis. These BTDA-TCNQ molecules are twisted with respect to each other by an angle of 66.1° defined by the least-square planes of respective aromatic rings in BTDA-TCNQ. To connect these twisted units, two types of $[Ru_2]$ units are present: $[\{Ru(1)\}_2]$ and $[\{Ru(2)\}_2]$ (Figure 2a) with an Ru(1)-N(1)-C(32) angle of 150.7(5)° and a Ru(2)-N(2)-C(34) angle of 156.9(5)°, in contrast to the essentially linear coordination mode found in **1** and **2**. The $Ru{-}N_{ax}$ (N_{ax} = cyano nitrogen atom of BTDA-TCNQ) distances are $d[Ru(1){-}N(1)] = 2.216(5)$ Å and $d[Ru(2){-}N(2)] = 2.264(5)$ Å in the two independent $[Ru_2]$ units. As a simple representation, the 3D network can be viewed as a "bundle of helical chains" of $\{\cdots[\{Ru(1)\}_2]$–(*syn*-TCNQ)–$[\{Ru(2)\}_2]$–(*syn*-TCNQ)–$[\{Ru(1)\}_2]$–(*cis*-TCNQ)–$[\{Ru(2)\}_2]$–(*cis*-TCNQ)$\cdots\}$ when projected along the a axis (Figure 2b and Figure S1, Supporting Information), where *syn*- and *cis*-TCNQ designations are used for BTDA-TCNQ molecules bridging through the 7,8- and 7,7-cyano groups, respectively; the two remaining cyano groups are engaged in the formation of adjacent chains. The neighboring $[Ru_2]\cdots[Ru_2]$ distances, which are defined as the distance between the midpoints of Ru–Ru bonds, are 10.37 Å for the *cis* bridges and 10.75 Å for the *syn* bridge in the same chain (these are $[\{Ru(1)\}_2]\cdots[\{Ru(2)\}_2]$) and 15.09 Å for the *trans* bridge $[\{Ru(1)\}_2]\cdots[\{Ru(1)\}_2]$ and 14.87 Å for the *trans* bridge $[\{Ru(2)\}_2]\cdots[\{Ru(2)\}_2]$ between chains via BTDA-TCNQ (Figure S1, Supporting Information). One CH_2Cl_2 molecule and a disordered area of 4-chlorotoluene/CH_2Cl_2 molecules with occupancy factors of 1.6/2.4 (as determined by X-ray crystallography) occupy the void space, resulting in a formula of $[\{Ru_2(O_2CPh\text{-}m\text{-}F)_4\}_2(\text{BTDA-TCNQ})]\cdot1.6(\text{4-chlorotoluene})\cdot3.4\,CH_2Cl_2$ for **3**. The disordered 4-chlorotoluene molecules are involved in π stacking interactions with both sides of the BTDA-TCNQ molecules at distances in the range of 3.25–3.44 Å.

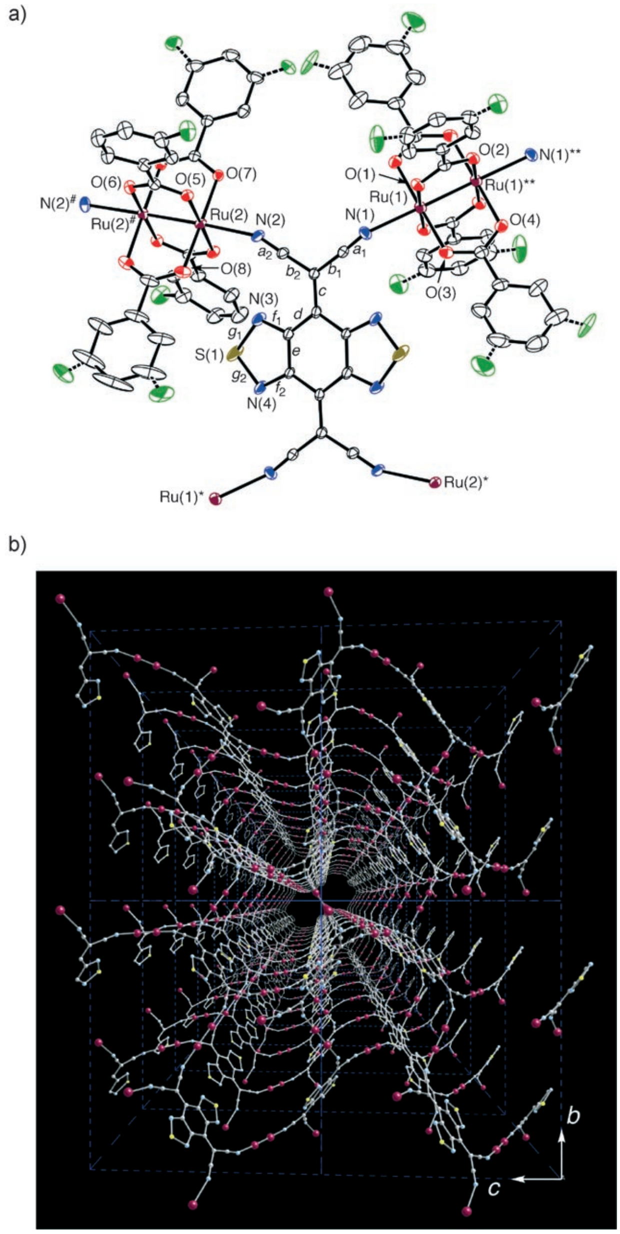

Figure 2. a) Thermal ellipsoid plot of the asymmetric unit (at 30% probability) and b) packing diagram projected along the a axis of **3**. Solvent molecules and m-$FPhCO_2$ ligands are omitted for clarity. Symmetry operations (*) $-x+3/2, -y+3/2, -z+1$; (#) $-x+1, y, -z+1/2$; (**) $-x+2, -y+1, -z+1$.

The bond lengths in the $[Ru_2]$ and BTDA-TCNQ moieties are helpful for assigning the degree of charge transfer from $[Ru_2]$ to BTDA-TCNQ. The nearly identical Ru–Ru distances 2.2734(6) (Ru(1)–Ru(1)*) and 2.2795(6) Å (Ru(2)–Ru(2)*) indicates that their oxidation states are indistinguishable. The $Ru{-}O_{eq}$ (O_{eq} = carboxylate oxygen) distance, however, is a sensitive probe of the oxidation state of the $[Ru_2]$ unit, and lies in the range of 2.07–2.09 Å for $[Ru_2^{II,II}]$ and 2.01–2.03 Å for $[Ru_2^{II,III}]$.[8] The average $Ru(1){-}O_{eq}$ and $Ru(2){-}O_{eq}$ distances are 2.031(4) and 2.060(4) Å, respectively. These data indicate that one-electron transfer from the two $[Ru_2]$ units has occurred, as the $[\{Ru(1)\}_2]$ and $[\{Ru(2)\}_2]$ units are respectively near to being $[Ru_2^{II,III}]$ and $[Ru_2^{II,II}]$ states. The bond lengths in the BTDA-TCNQ moiety of **3** are listed in Table S1 (Supporting Information) together with those of BTDA-TCNQ salts reported previously.[13,14,15,16] As was observed in previously studied compounds, the difference in bond lengths for BTDA-TCNQ (from 0 to −1) are very small, but a rough trend can still be observed, as in the case of TCNQ: b and d are shortened and meanwhile c and e (b–d are defined in Figure 2a and Table S1, Supporting Information) are lengthened on increasing the charge from 0 to −1; in particular, the distance c is characteristic. Therefore, the oxidation state of BTDA-TCNQ was evaluated by three relationships based on c: $\rho_c = A_1c + B_1$, $\rho_{c/d} = A_2c/d + B_2$, $\rho_{c/(b+d)} = A_3[c/(b+d)] + B_3$ (Kistenmacher relationship),[17] on the basis of neutral BTDA-TCNQ ($\rho = 0$)[13] and [NEt(Me)$_3$]BTDA-TCNQ ($\rho = -1$)[16] with $A_1 = -25.64$, $B_1 = 34.64$, $A_2 = -22.73$, $B_2 = 20.98$, $A_3 = -50.00$, and $B_3 = 23.25$. The estimated values for **3** are $\rho_c = -1.435$, and $\rho_{c/d} = -1.463$, and $\rho_{c/(b+d)} = -1.512$ (Table S1, Supporting Information). The values estimated for previous compounds tend to be $+0.1$ to $+0.3$ larger than the expected value. Hence, the BTDA-TCNQ moiety in **3** is close to being a fully reduced monoanion, but might be slightly more oxidized, which would imply a noninteger charge-polarized state of $[\mathrm{Ru_2}^{5+}]$–$[\text{BTDA-TCNQ}^{(1+\delta)-}]$–$[\mathrm{Ru_2}^{(4+\delta)+}]$ ($\delta \approx 0.1$–0.4).

Field-cooled dc magnetic susceptibility (FCM) measurements were performed on a polycrystalline sample of **3** at 1 kOe in the temperature range of 1.8–300 K; χ and χT are plotted in Figure 3 a as a function of temperature. The χT value of 3.54 cm^3 K mol^{-1} at 300 K is much larger than the spin-only value of 2.00 cm^3 K mol^{-1} ($g = 2.00$) expected for two isolated $[\mathrm{Ru_2}^{4+}]$ units with $S = 1 \times 2$ (as BTDA-TCNQ^0), a clear indication of electron transfer from the $[\mathrm{Ru_2}^{4+}]$ units to BTDA-TCNQ and significant interactions between magnetic centers even at high temperatures. The χT value increases gradually on cooling to about 110 K (15.6 cm^3 K mol^{-1}) and then steeply increases below this temperature to reach a maximum value of 590 cm^3 K mol^{-1} at 76 K, followed by a decrease to 19.2 cm^3 K mol^{-1} at 1.8 K. The χ value also shows a sudden increase at around 110 K with no peak appearing until 1.8 K, which suggests the onset of long-range ferromagnetic ordering. The $1/\chi$ versus T plot is nearly linear in the paramagnetic region above 110 K with Curie and Weiss constants of 2.34 cm^3 K mol^{-1} and 99 K, respectively (Figure S2, Supporting Information). The large positive Weiss constant supports strong coupling between magnetic centers through the $[\mathrm{Ru_2}^{5+}]$–$[\text{BTDA-TCNQ}^{(1+\delta)-}]$–$[\mathrm{Ru_2}^{(4+\delta)+}]$ unit. Note that the obtained Curie constant seems to be rather close to the spin-only value for two isolated $[\mathrm{Ru_2}^{4+}]$ units with neutral BTDA-TCNQ, but such a discussion on constitutive spins from this value should be avoided given the existence of such strong magnetic coupling.

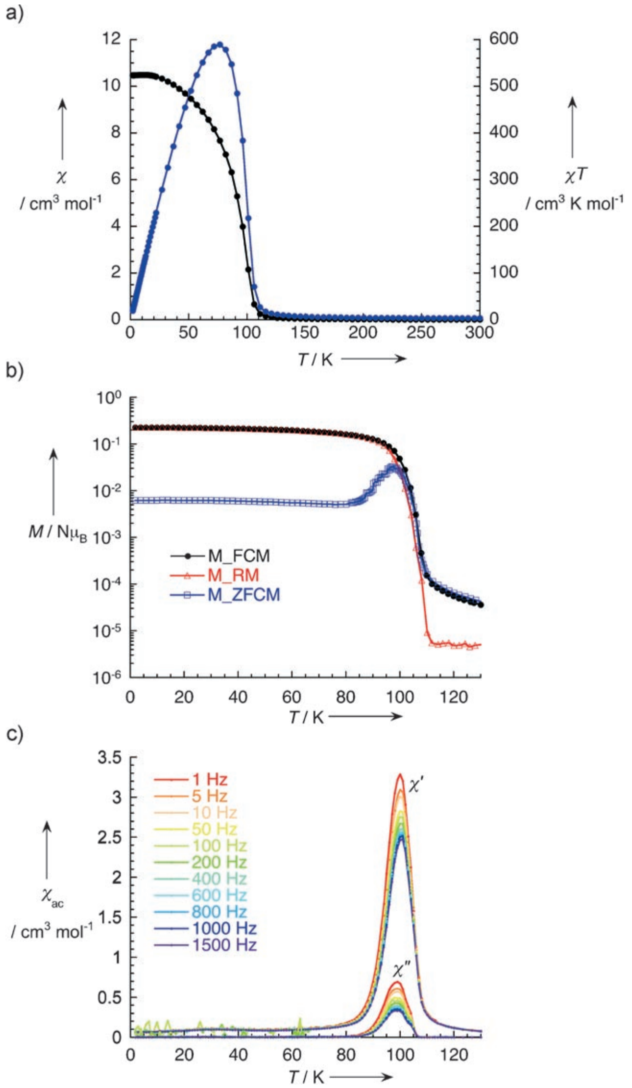

Figure 3. a) Temperature dependence of χ and χT at 1 kOe; b) FCM, RM, and ZFCM at 3 Oe; c) ac susceptibilities χ' (in-phase) and χ'' (out-of-phase) at zero dc field and 3 Oe ac oscillating field for **3**.

To confirm the existence of long-range ferromagnetic ordering, low-field magnetization was measured at 3–100 Oe (see Figure 3 b for 3 Oe). Even at such low fields, the FCM begins to abruptly increase at 110 K with no cusp appearing until 1.8 K in any applied field, evidence of the presence of long-range ferromagnetic order. Remnant magnetization (RM) tracks the FCM curve and disappears at 110 K. The zero-field cooled magnetization (ZFCM) curve exhibits a peak at 98 K, but traces the FCM curve above 107 K. Finally, ac magnetic susceptibility data at zero dc field and 3 Oe ac oscillating field in the frequency range of 1–1500 Hz (Figure 3 c) were measured. Both χ' and χ'' versus T plots show a peak at 100 K and χ'' begins to increase at 107 K (T_c). It should be noted that a frequency dependence of susceptibility, but no shift of the maximum, is observed for both χ' and χ''.

Figure 4 shows hysteresis loops measured at several temperatures (Figure S3, Supporting Information). On the

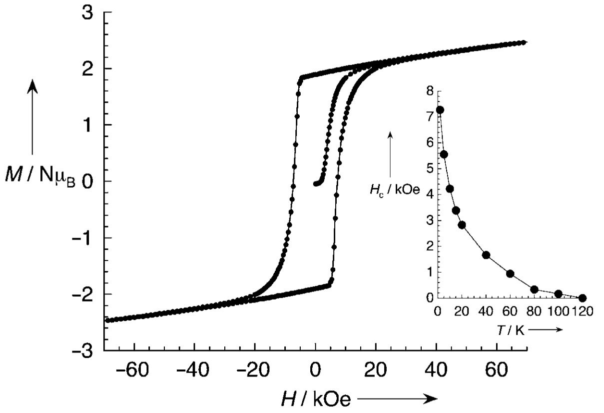

Figure 4. Field dependence of the magnetization of **3** at 1.82 K. Inset: temperature dependence of the coercive field H_c.

initial sweep of field, the magnetization M shows a resistive response rather than a smooth one on applying low fields, typical for hard magnets (in good agreement with the low-field ZFCM data). Indeed, coercive fields were detected until 100 K (7250 Oe at 1.8 K; inset of Figure 4). The magnetization at 7 T is $M_s = 2.47\ \mu_B$ at 1.8 K, which is much smaller than any total spin state (S_T) that is possible for the unit $[\mathrm{Ru_2}^{5+}]$–[BTDA-TCNQ$^{\bullet-}$]–$[\mathrm{Ru_2}^{4+}]$: $S_T = (3/2+1/2+1) = 3$ (ferromagnetic arrangement; 6.00 μ_B), $S_T = (1/2+1/2+1) = 2$ (ferromagnetic arrangement; 4.00 μ_B), or $S_T = (3/2-1/2+1) = 2$ (ferrimagnetic arrangement; 4.00 μ_B).[18] This could be due to large anisotropy arising from the [Ru$_2$] units.[8] A linear increase of M with increasing field supports this hypothesis.

In conclusion, a new structural type of D$_2$A charge-transfer system with a 3D structure has been isolated from the self-assembly of [Ru$_2$(O$_2$CPh-*m*-F)$_4$] with BTDA-TCNQ. The present compound exhibits long-range ferromagnetic order with $T_c = 107$ K. Nevertheless, a charge-localized state is dominant despite the essentially full electron-transfer from [Ru$_2$] to BTDA-TCNQ.[19] The high T_c in this 3D compound and the T_N of 95 K for related 2D compound **2**,[11] however, make these types of materials promising targets for future exploration of π–d D$_2$A systems in which magnetic ordering and conductivity coexist. To achieve this goal, the design of highly symmetrical structures that lead to identical donor D units in a D$_2$A system is crucial, and, if successful, should lead to a much higher T_c based on the double-exchange mechanism.

Experimental Section

Synthesis of **3**: All synthetic procedures were carried out under anaerobic conditions. Diruthenium(II,II) compound [Ru$_2$(O$_2$CPh-*m*-F)$_4$(thf)$_2$] was prepared by adaptation of a literature procedure.[20] A solution of [Ru$_2$(O$_2$CPh-*m*-F)$_4$(thf)$_2$] (181 mg, 0.20 mmol) in CH$_2$Cl$_2$ (25 mL) was separated into 1-mL portions and placed in narrow diameter sealed glass tubes (∅ 8 mm). A solution of BTDA-TCNQ (33 mg, 0.1 mmol) of 4-chlorotoluene (75 mL) was carefully placed in 3-mL portions onto each CH$_2$Cl$_2$ layer, and slow diffusion was allowed to occur. The glass tubes were left undisturbed for a week or more to yield block-shaped, dark green crystals of **3**. Yield: 26%. Elemental analysis (%) calcd for **3**·1.6(4-chlorotoluene)·3CH$_2$Cl$_2$ C$_{82.60}$H$_{50}$N$_8$O$_{16}$Cl$_{8.40}$F$_8$Ru$_4$S$_2$: C 42.60, H 2.16, N 4.81; found: C 43.10, H 2.25, N 5.13; IR (KBr): $\tilde{\nu}$(C≡N), 2196, 2134 cm^{-1}.

Crystal data for **3**: C$_{82.60}$H$_{50}$N$_8$O$_{16}$Cl$_{8.40}$F$_8$Ru$_4$S$_2$, FW = 2328.74, monoclinic *C2/c* (no. 15), $T = 93 \pm 1$ K, $\lambda(\mathrm{Mo_{K\alpha}}) = 0.71070$ Å, $a = 17.481(3)$, $b = 24.505(3)$, $c = 21.049(3)$ Å, $\beta = 92.995(2)°$, $V = 9004(2)$ Å^3, $Z = 4$, $\rho_{\mathrm{calcd}} = 1.718$ g cm^{-3}, $F_{000} = 4609.60$, $2\theta_{\max} = 53.0°$. Final $R1 = 0.0684$ ($I > 2.00\sigma(I)$), $R1 = 0.0870$ (all data), $wR2 = 0.1791$ (all data), GOF = 1.003 for 632 parameters and a total of 35674 reflections, 10290 unique ($R_{\mathrm{int}} = 0.080$). The linear absorption coefficient μ for Mo$_{K\alpha}$ radiation was 10.388 cm^{-1}. An empirical absorption correction was applied and resulted in transmission factors ranging from 0.521 to 0.771, which were corrected for Lorentzian and polarization effects. Maximum positive and negative peaks in the ΔF map were $\rho_{\max} = 2.31$ e Å^3 and $\rho_{\min} = -1.74$ e Å^3. CCDC 689769 contains the supplementary crystallographic data for this paper. These data can be obtained free of charge from The Cambridge Crystallographic Data Centre via www.ccdc.cam.ac.uk/data_request/cif.

Received: June 3, 2008
Revised: July 8, 2008

Keywords: carboxylate ligands · electron transfer · magnetic properties · quinodimethanes · ruthenium

---

[1] C. Creutz, H. Taube, *J. Am. Chem. Soc.* **1969**, *91*, 3988.

[2] a) C. Creutz, H. Taube, *J. Am. Chem. Soc.* **1973**, *95*, 1086; b) G. M. Tom, C. Creutz, H. Taube, *J. Am. Chem. Soc.* **1974**, *96*, 7827; c) M. J. Powers, D. J. Salmon, R. W. Callahan, T. J. Meyer, *J. Am. Chem. Soc.* **1976**, *98*, 6731.

[3] a) N. S. Hush, *Trans. Faraday Soc.* **1961**, *57*, 155; b) N. S. Hush, *Prog. Inorg. Chem.* **1967**, *8*, 391.

[4] R. A. Marcus, N. Sutin, *Biochim. Biophys. Acta Nucleic Acids Protein Synth.* **1985**, *95*, 8198.

[5] K. D. Demadis, C. M. Hartshorn, T. J. Meyer, *Chem. Rev.* **2001**, *101*, 2655, and references therein.

[6] M. A. S. Aquino, F. L. Lee, E. J. Gabe, C. Bensimon, J. E. Greedan, R. J. Crutchley, *J. Am. Chem. Soc.* **1992**, *114*, 5130.

[7] M. B. Robin, P. Day, *Adv. Inorg. Chem. Radiochem.* **1967**, *10*, 247.

[8] a) F. A. Cotton, R. A. Walton, *Multiple Bonds Between Metal Atoms*, 2nd ed., Oxford University Press, Oxford, **1993**; b) *Multiple Bonds Between Metal Atoms*, 3rd ed. (Ed.: F. A. Cotton, C. A. Murillo, R. A. Walton), Springer, New York, **2005**.

[9] a) H. Miyasaka, R. Clérac, C. S. Campos-Fernández, K. R. Dunbar, *J. Chem. Soc. Dalton Trans.* **2001**, 858; b) S. Furukawa, M. Ohba, S. Kitagawa, *Chem. Commun.* **2005**, 865.

[10] H. Miyasaka, C. S. Campos-Fernández, R. Clérac, K. R. Dunbar, *Angew. Chem.* **2000**, *112*, 3989; *Angew. Chem. Int. Ed.* **2000**, *39*, 3831.

[11] H. Miyasaka, T. Izawa, N. Takahashi, M. Yamashita, K. R. Dunbar, *J. Am. Chem. Soc.* **2006**, *128*, 11358.

[12] N. Motokawa, T. Oyama, S. Matsunaga, H. Miyasaka, K. Sugimoto, M. Yamashita, N. Lopez, K. R. Dunbar, *Dalton Trans.* **2008**, *31*, 4099.

[13] T. Suzuki, H. Fujii, Y. Yamashita, C. Kabuto, S. Tanaka, M. Harasawa, T. Mukai, T. Miyashi, *J. Am. Chem. Soc.* **1992**, *114*, 3034.

[14] T. Suzuki, C. Kabuto, Y. Yamashita, T. Mukai, *Bull. Chem. Soc. Jpn.* **1987**, *60*, 2111.

[15] K. Iwasaki, A. Ugawa, A. Kawamoto, Y. Yamashita, K. Yakushi, T. Suzuki, T. Miyashi, *Bull. Chem. Soc. Jpn.* **1992**, *65*, 3350.

[16] T. Suzuki, C. Kabuto, Y. Yamashita, T. Mukai, T. Miyashi, G. Saito, *Bull. Chem. Soc. Jpn.* **1988**, *61*, 483.

[17] T. J. Kistenmacher, T. J. Emge, A. N. Bloch, D. O. Cowan, *Acta Crystallogr. Sect. B* **1982**, *38*, 1193.

[18] $S_T = (1/2-1/2+1) = 1$ (ferrimagnetic arrangement; 2.00 μ_B) might be also possible assuming a large g value. However, the linear increase of magnetization versus H even at 7 T suggests that saturation of magnetization occurs at a much higher value than 2.47 μ_B at 7 T, i.e., $g > 2.47$. Such a g value would be excluded in the family of diruthenium compounds.

[19] Direct-current conductivity data were measured on a single crystal of **3** by the two-probe method in the temperature range of 4–300 K (Figure S4, Supporting Information). The conductivity at room temperature of $\sigma = 9.7 \times 10^{-5}$ S cm^{-1}, measured with the probes attached along the a axis, decreases continuously on cooling, and finally insulator behavior is observed below about 180 K (no anomaly was observed until 4 K). This behavior is almost the same as with heating. The Arrhenius plot of ρ shows a linear dependence above 180 K with an activation energy $E_a = 358$ meV, indicating semiconducting behavior.

[20] S. Furukawa, S. Kitagawa, *Inorg. Chem.* **2004**, *43*, 6464.